

Article

Design and Validation of Pitch H-Infinity Controller for a Large Wind Turbine

Yuan Song ¹, Taesu Jeon ², Insu Paek ^{2,3,*} and Bayasgalan Dugarjav ⁴

¹ Department of Advanced Mechanical Engineering, Kangwon National University, Chuncheon-si 24341, Gangwon, Republic of Korea

² Department of Integrated Energy & Infra System, Kangwon National University, Chuncheon-si 24341, Gangwon, Republic of Korea

³ Department of Mechatronics Engineering, Kangwon National University, Chuncheon-si 24341, Gangwon, Republic of Korea

⁴ Department of Electronics and Communication Engineering, School of Engineering and Applied Sciences, National University of Mongolia, Ulaanbaatar 14201, Mongolia

* Correspondence: paek@kangwon.ac.kr; Tel.: +82-33-250-6379

Abstract: In this study, a pitch H-infinity control algorithm was developed for variable-speed-variable-pitch (VSVP) wind turbines to improve the rotor standard deviation of the wind turbines under normal and extreme wind conditions. The pitch H-infinity control algorithm only uses H-infinity control in the blade pitch control loop in the rated power region, and conventional torque gain scheduling algorithms are applied in the partial power region. The performance of this controller was verified using simulations of a 5 MW wind turbine using the commercial aeroelastic simulation code Bladed. The performance of the pitch H-infinity controller was compared with that of the conventional proportional-integral (PI) control algorithm under three different operating conditions: normal operating conditions without sensor noise, normal operating conditions with sensor noise, and extreme operating conditions without sensor noise based on the wind turbine design standard by IEC. Based on the simulation results with two different wind speed regions, namely, the transition region and the rated power region, it was found that the proposed pitch H-infinity controller showed better rotor speed standard deviation performance in the three operating conditions and achieved lower standard deviations of the rotor speed and the electrical power without affecting the mean electrical power.

Keywords: H-infinity control algorithm; robust control; proportional-integral (PI) control; gain scheduling; normal turbulence model (NTM); extreme operating gust (EOG); sensor noise interference; wind estimator



Citation: Song, Y.; Jeon, T.; Paek, I.; Dugarjav, B. Design and Validation of Pitch H-Infinity Controller for a Large Wind Turbine. *Energies* **2022**, *15*, 8763. <https://doi.org/10.3390/en15228763>

Academic Editor: Taimoor Asim

Received: 4 October 2022

Accepted: 17 November 2022

Published: 21 November 2022

Publisher's Note: MDPI stays neutral with regard to jurisdictional claims in published maps and institutional affiliations.



Copyright: © 2022 by the authors. Licensee MDPI, Basel, Switzerland. This article is an open access article distributed under the terms and conditions of the Creative Commons Attribution (CC BY) license (<https://creativecommons.org/licenses/by/4.0/>).

1. Introduction

The levelized cost of electricity (LCOE) of onshore wind has been gradually reduced and is known to be even lower than the conventional power generation technologies using coal and gas in many countries [1]. This trend is expected to continue in the future, because the LCOE of conventional technologies rises due to increases in CO₂ certificate prices, but the LCOE of the onshore wind is expected to decrease with technological developments [1].

To reduce the LCOE of wind technology, wind turbines are becoming larger. This increases the tower height and the rotor diameter of the wind turbines. Larger wind turbines with higher hub heights and larger rotor diameters are subjected to operation in more severe wind conditions due to the higher mean wind speed and larger wind shear between the highest and lowest blade tip positions in operation, and this renders the wind turbines vulnerable to noise due to vibration [2,3]. Therefore, for larger wind turbines, more stable and robust control algorithms are needed, not only to ensure the demanded power output in noise-free environments but also to ensure stable power output with a load reduction in a noisy environment.

Multi-megawatt wind turbines are variable-speed–variable-pitch (VSVP) machines and only have three different power generation regions according to their rated wind speeds in normal operation: a maximum power coefficient region at low wind speeds, a transition region near the rated wind speed, and a rated power region at high wind speeds [4]. The maximum power coefficient region is characterized by the generator torque control of a wind turbine to achieve the maximum power coefficient at varying wind speeds. In this region, wind turbines produce power that is lower than their rated values with the highest aerodynamic rotor efficiency. The rated power region is characterized by the blade pitch control to maintain the rated power, even under wind speeds higher than the rated value. In this region, wind turbines are controlled to maintain the rated power as long as the wind speed is higher than the rated wind speed. The transition region is the region in between the maximum power region and the rated power region, and it ensures a smooth transition between the two.

To fulfill the power control for different power generation regions, conventional algorithms for single-input–single-output (SISO) systems have been selected for commercial multi-megawatt wind turbines, which consist of two control loops: one for the generator torque and the other for the blade pitch angle. For the maximum power coefficient region, the blade pitch angle is fixed to the fine pitch angle of the given rotor, and to maximize the power coefficient, the generator torque is directed to the generator through the power converter using a precalculated look-up table with an input of generator speed and an output of generator torque. For the rated power region, the constant rated generator torque or the varying torque of the measured power divided by the measured generator speed is directed to the generator. Moreover, a closed-loop PI or PID control algorithm is used to minimize the error between the rated generator speed and the measured one, and the controller output is directed to the blade pitch actuators [5–7].

For load reduction algorithms to be applied to conventional wind turbine power control algorithms, additional control loops for specific purposes need to be added. Such load reduction algorithms include individual pitch control (IPC), tower damper, and feed-forward blade pitch control [8–13]. In [8], it was shown that the IPC control algorithm can reduce flap-wise blade loading and nacelle loading. In [9], two control strategies (IPC and collective pitch control (CPC)) were designed for the NREL 5 MW wind turbine. The results showed that the IPC control algorithm can reduce blade loads under above-rated wind speed conditions compared to the CPC control algorithm. In [10], the IPC gain scheduling algorithm (IPS) was designed based on the IPC control algorithm to achieve the effect of tower load reduction. The simulation results showed that the IPS algorithm can reduce the tower for-aft moment by up to 14% compared to the conventional IPC control algorithm. In [11], the angular acceleration of the nacelle was used as a feedback control loop to design a tower damper in order to reduce the load on the floating wind turbine. In [12], a tower damper was designed for a medium-capacity wind turbine. The simulation results showed that the tower root for-aft load was reduced by 9.7% to 32.0%. In [13], a gain scheduling tower damper using the measured blade pitch angle feedback signal was designed based on the conventional tower damper algorithm. The simulation results showed that the maximum load reduction was 7.9% for the tower root for-aft load compared with the conventional tower damper algorithm.

Due to the uncertainty of wind turbine models and operating environments, robust control techniques have been investigated for application to wind turbines in order to achieve better stability [14–18]. In [14], a DK-iterative algorithm-based H-infinity controller was designed for a wind turbine model with uncertainty, and a simulation was performed using MATLAB. It was found from the simulation that the proposed H-infinity control can reduce the pitch angle oscillation resulting from the model uncertainty and that it can maintain robustness. In [15], assuming the case of blade mass increase due to blade icing, an H-infinity controller was designed and verified in a simulation by modeling the uncertainty of a wind turbine. In the simulation, the proposed controller showed greater robustness to disturbances in cold environments than the conventional PI control. In [16], a

multi-input–single-output (MISO) H-infinity controller was designed for a wind turbine to be used in the rated power region. It was found from a simulation in normal and extreme wind conditions that the proposed controller could reduce the load on the wind turbine. A linear matrix inequality (LMI) was introduced in [17] to obtain a suboptimal solution to the optimization problem of H2/H-infinity controllers to better suppress oscillations under disturbance conditions by adding a power oscillation damper. In [18], a linear parameter varying (LPV) H-infinity controller based on the LMI method was designed to achieve better performance than the PID controller.

Although previous studies have shown the robustness of H-infinity control for wind turbines under model uncertainty conditions using simulations, there still exist a few limitations. First of all, the mean power and rotor standard deviation of the H-infinity controller under sensor noise interferences in the input signals to the controller that might arise in reality have not been fully verified.

The second limitation is that most H-infinity studies use simplified numerical wind turbine models constructed by the authors, and, therefore, large discrepancies between the numerical model used for simulation (or validation) and the wind turbine in reality might exist. The third limitation is that, in most studies, the H-infinity control in the rated power region of the pitch control was designed and validated without considering the coupling effect of the pitch and torque control in the transition region, which may lead to degradations in the mean power and rotor standard deviation of wind turbines in the transition region. Moreover, this is important in order for the proposed control to be implemented in an actual wind turbine for experimental validation.

Therefore, in this study, H-infinity robust control is revisited, but a new hybrid algorithm to achieve the robustness of H-infinity control and to partially utilize the current conventional control of wind turbines in consideration of actual implementation is proposed. More specifically, a pitch H-infinity control algorithm is designed to improve the rotor standard deviation of wind turbines under normal and extreme wind conditions. The performance of the proposed H-infinity controller is verified using dynamic simulations with the commercial aeroelastic analysis code Bladed in noiseless and noise conditions, and it is also compared with the performance of a conventional controller.

2. Target Wind Turbines

In this study, the wind turbine used for simulation is an offshore wind turbine with a rated power of 5 MW, designed by the National Renewable Energy Laboratory (NREL) for use in research. The specifications of the wind turbine are shown in Table 1 [19].

Figures 1 and 2 show an image of the NREL 5 MW wind turbine and its steady power curve, respectively. As shown in Figure 2, the power curve can be divided into three regions, namely, the maximum power coefficient region below the rated wind speed, the rated power region above the rated wind speed, and the transition region in between.

In this study, the target wind turbine was modeled and simulated using Bladed (version 4.6), a commercial aeroelastic simulation code for wind turbines. The structural and material property information of the wind turbine blades, drive train, tower, and nacelle were imported into Bladed to construct a nonlinear model of the NREL 5 MW wind turbine.

Table 1. General specifications of target wind turbines.

Specification	NREL	Unit
Rated power	5×10^6	W
Rotor diameter	126	m
Hub height	90	m
Rated rotor speed	12.1	rpm
Cut-in/rated/cut-off	3/11.4/25	m/s
Wind speed		
TSR	7.00	-

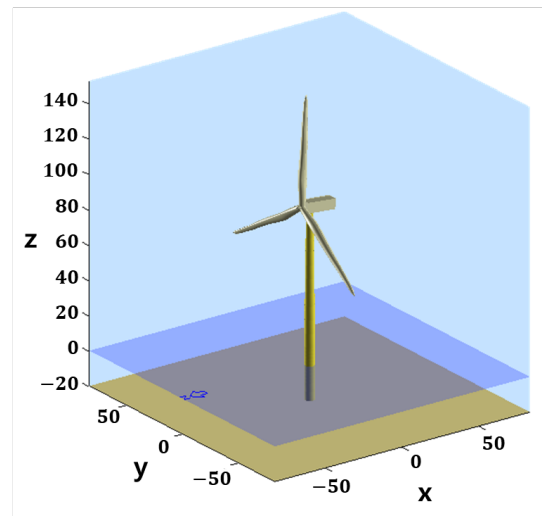


Figure 1. Images of the target NREL 5 MW large wind turbine.

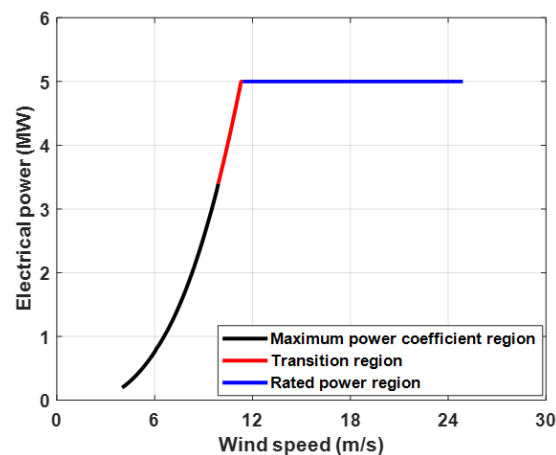


Figure 2. The power curve of the target wind turbine.

3. Control Algorithms

3.1. PI Control Algorithm

A conventional PI control algorithm was used in this study as a baseline control algorithm for comparison with the proposed H-infinity control algorithm. The PI control algorithm in this study uses three feedback signals, namely, the pitch angle, the electrical power, and the generator speed, as inputs to the controller, and it sends the pitch angle and the torque commands to the target wind turbine. The baseline PI control algorithm only has power control algorithms and does not include any additional load reduction algorithms available in the literature [9–13,20].

Figure 3 shows a block diagram of the PI control algorithm. As shown in the figure, the PI control algorithm consists of two modules for the blade pitch angle and the generator torque controls, as well as a mode switch.

The input signals of the controller are the output signals of the wind turbine, which are the generator speed (Ω_g), the blade pitch angle (β), and the electrical power (P). The blade pitch command (β_c) and the generator torque command (T_g^c) are the command signals, which are calculated using the PI control algorithm.

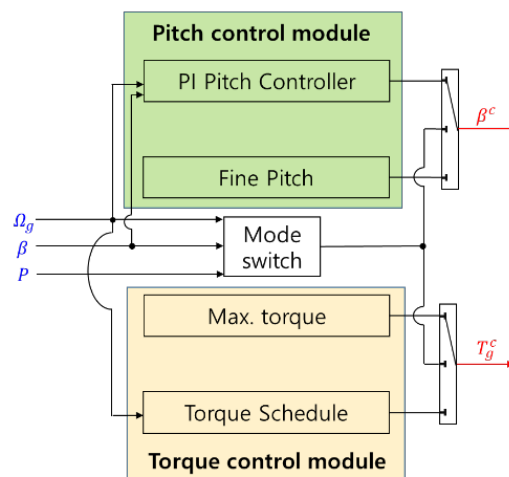


Figure 3. Block diagram of the PI control algorithm.

In the maximum power coefficient region, the control strategy aims to maintain the optimal power coefficient (C_p) in order to maximize the power output. For this, the blade pitch angle is fixed to the fine pitch angle, and the generator torque is adjusted based on the measured generator speed to achieve the optimal speed ratio. In this study, a look-up table using the generator speed as the input and the generator torque as the output was constructed based on a steady-state analysis to achieve the optimal tip speed, and it was used for the generator torque command. The look-up table is shown in Figure 4. The two linear lines at both ends of the nonlinear curve represent the two transition regions for starting and the smooth connection to the rated power region.

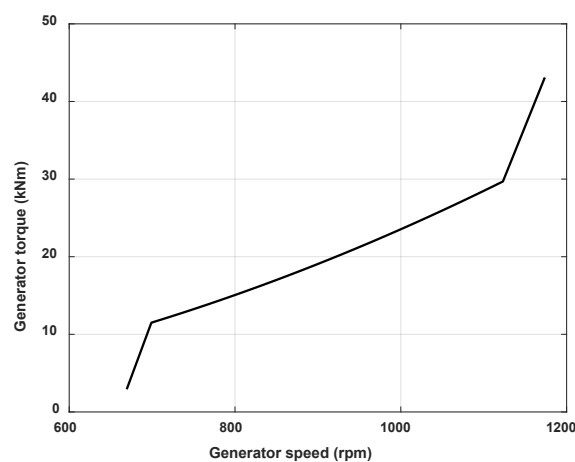


Figure 4. A look-up table curve between the generator speed and generator torque.

In the rated power region, the control strategy is to maintain the rated power of the target wind turbine by adjusting the pitch angle of the blades. For this, the generated torque is fixed to the rated value, and a PI control algorithm is used to adjust the blade pitch angle to minimize the error between the rated generator speed and the measured generator speed.

For switching the control strategies of the maximum power coefficient region, including the transition regions and the rated power region, an SR flip-flop mode switch with the inputs of pitch angle, generator power, and generator speed is used. The pitch PI control algorithm in the rated power region is used when the SR flip-flop mode switch is activated,

and the look-up-table-based gain-scheduling algorithm in both the maximum power region and the transition region is used when the SR flip-flop mode switch is deactivated.

3.2. H-Infinity Control Algorithm of Mixed Sensitivity

The H-infinity control algorithm requires certain performance levels in the disturbance signals, sensor noise signals, and unmodeled plant dynamics, thus introducing the need for sensors to ensure the stability of the system. Therefore, in this study, mixed sensitivity optimization is solved to achieve the optimization of the H-infinity controller and to ensure the stability of the wind turbine.

The standard control problem can be considered as designing the controller K according to a plant G to achieve closed-loop stability. In the H-infinity control algorithm, the weighting functions W_p , W_u , and W_m are attached to the system with the purpose of considering tracking, controller adjustment, sensor noise, wind speed uncertainties, and model uncertainties. A block diagram of the H-infinity control algorithm with the mixed sensitivity function is shown in Figure 5.

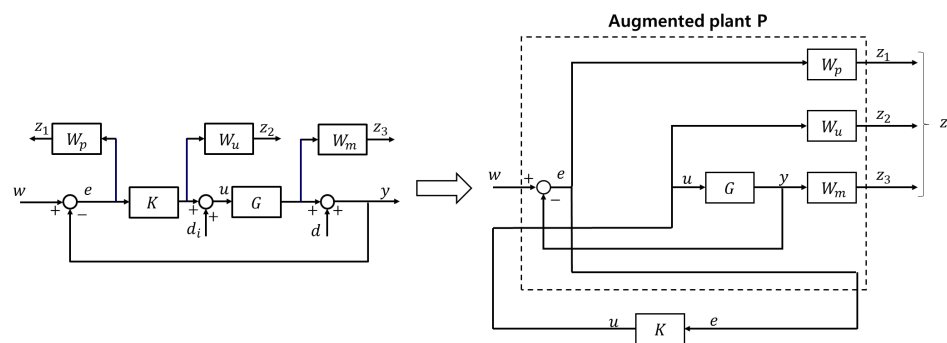


Figure 5. Block diagram of the H-infinity control algorithm with mixed sensitivity.

The variables w , e , u , y , d , and d_i are the reference input, tracking error, control output, system output, output disturbance, and the input disturbance, respectively. W_p , W_u , and W_m are the weighting functions of the sensitivity function S , the control effort KS , and the complementary sensitivity function T , respectively. The system plant, the augmented plant, and the controller are denoted by G , P , and K , respectively. The transfer function $M(s)$ from w to z can be expressed as Equation (1):

$$M(s) = \begin{bmatrix} W_p S \\ W_u K S \\ W_m T \end{bmatrix} \quad (1)$$

The H-infinity controller is designed to obtain the controller K by selecting the appropriate weighting functions W_p , W_u , and W_m under the condition of considering the input disturbance d and output disturbance d_i . Additionally, it satisfies the Equation (1) $\|M(s)\|_\infty$ minimization while ensuring the closed-loop stability of the system. Moreover, the controller K should satisfy the condition that the sensitivity function, control effort, and complementary sensitivity function are smaller than the weighting functions $1/W_p$, $1/W_u$, and $1/W_m$, respectively, as shown in Equation (2):

$$S \leq |W_p^{-1}|, KS \leq |W_u^{-1}|, T \leq |W_m^{-1}| \quad (2)$$

where the sensitivity function S is related to plant G and controller K , as shown in Equation (3). The sensitivity function is introduced to improve the tracking of the reference signal and the ability to suppress external disturbances. KS represents the ability to suppress the

saturation of the controller output. The complementary sensitivity function is introduced to ensure the robust stability of the system.

$$S = (I + GK)^{-1}, T = (I - S) = GK(I + GK)^{-1} \tag{3}$$

The weighting functions W_p , W_u , and W_m are chosen as low-pass filters and high-pass filters, and they are defined as shown in Equations (4) and (5) [21]:

$$W_p = \frac{\frac{s}{M_p} + \omega_p}{s + \omega_p \epsilon_p} \tag{4}$$

$$W_{u,m} = \frac{s + \frac{\omega_{u,m}}{M_{u,m}}}{\epsilon_{u,m}s + \omega_{u,m}} \tag{5}$$

3.3. Pitch H-Infinity Control Algorithm

Figure 6 shows a block diagram of the pitch H-infinity control algorithm. As with the conventional PI control algorithm, the pitch H-infinity control algorithm consists of a pitch control module, a torque control module, and a mode switch. The pitch H-infinity control algorithm has five inputs, which are the generator speed (Ω_g), the blade pitch angle (β), the electrical power (P), the generator torque (T_g), and the fore-aft acceleration of the tower ($T_{W_{fa}}$). In the pitch control module, the wind speed is needed to obtain the real-time state reference of the wind turbine, and the H-infinity control algorithm is used to control the pitch angle of the wind turbine in the rated power region. The generator torque is fixed to the maximum torque (rated generator torque), which is the same as the conventional PI control.

With the exception of the pitch control loop in the rated power region, all the other algorithms are the same as those in the conventional PI control, and this allows the proposed algorithm to be easily implemented in conventional technology. However, the pitch actions with the proposed H-infinity algorithm in the rated power region are different from the pitch actions with the conventional PI algorithm, and this entails changes in switching actions with the mode switch and results in the behavior in the transition region being slightly different from that of the conventional PI algorithm.

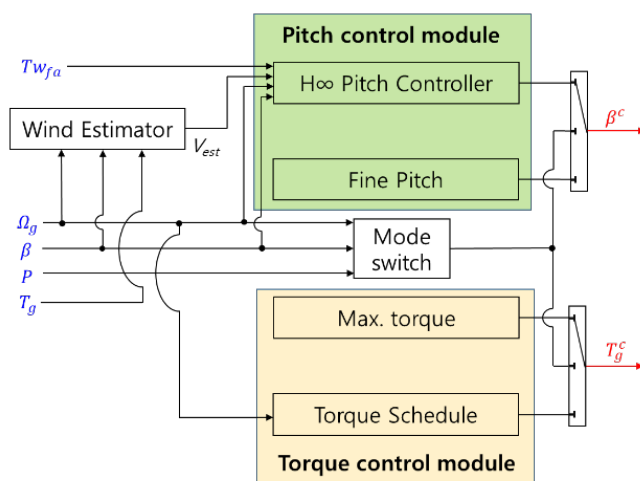


Figure 6. Block diagram of the pitch H-infinity control algorithm.

3.4. Wind Estimator

The pitch H-infinity controller needs to control the wind turbine using real-time reference values of the generator speed, pitch angle, and generator torque. These reference

values are directly related to the wind speed, and, therefore, real-time wind speed data are required as input to the controller.

In this study, a wind estimation module is used to calculate the real-time wind speed data needed. Figure 7 shows a block diagram of the wind estimation module, which consists of a low-pass filter for rotor speed, an aerodynamic torque estimator, and a 3D look-up table [22].

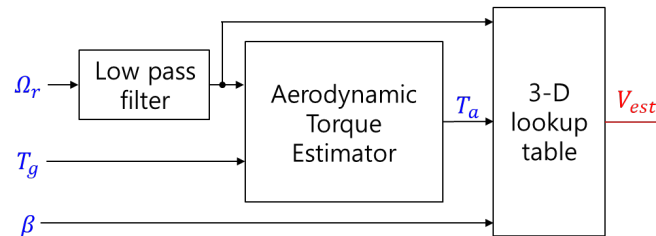


Figure 7. Block diagram of wind estimator.

The low-pass filter of the wind estimator module is aimed at filtering the high-frequency sensor noise in the rotor speed data from the wind turbine. The aerodynamic torque estimator module is the inverse of the two-mass drive-train model to estimate the aerodynamic torque, and the equations are shown in Equations (6) and (7):

$$(J_r + J_g) \frac{d\Omega_r}{dt} = J_t \frac{d\Omega_r}{dt} = J_t \frac{d\Omega_g}{dt} = T_a - T_g, \quad (6)$$

$$T_a = (J_r + J_g) \frac{d\Omega_r}{dt} + T_g, \quad (7)$$

where J is the moment of inertia, Ω is the rotational speed, T_a is the aerodynamic torque, T_g is the generator reaction torque, r is the index referring to the rotor, and g is the index referring to the generator.

The filtered rotor speed signal, the aerodynamic torque evaluated using the equations, and the pitch angle signal are used as inputs to a 3D look-up table to calculate the estimated wind speed.

The 3D look-up table is generated using MATLAB through a function minimization algorithm [22], which minimizes the error between the trial aerodynamic torque and the rated aerodynamic torque. To calculate the trial aerodynamic torque, Equation (8) is used, where the air density (ρ) and rotor radius (R) are constant values. C_Q is the torque coefficient, which is the 3D look-up table calculated by the software Bladed with respect to the tip speed ratio (λ) and the blade pitch angle (β). The tip speed ratio is calculated as shown in Equation (9), and it is related to the rotor speed (Ω_r) and wind speed (V).

Therefore, the rotor speed, blade pitch angle, and wind speed are used as inputs to calculate the trial aerodynamic torque. Moreover, the error between the trial aerodynamic torque and the rated aerodynamic torque is used as a cost function, and the minimum of the function is the corresponding wind speed value.

$$T_a = \frac{1}{2} \rho \pi R^3 C_Q(\lambda, \beta) V^2 \quad (8)$$

$$\lambda = \frac{\Omega_r R}{V} \quad (9)$$

4. Simulation

4.1. Method

The simulation was performed with two different control algorithms, namely, the conventional PI and the proposed pitch H-infinity. MATLAB/Simulink was used to compile

the control algorithm into a dynamic link library (DLL), and the compiled DLL was implemented in the Bladed program as an external controller for dynamic simulations.

To verify the performance of the controller in multiple wind speed regions, two different mean wind speeds—one for the transition region (12 m/s) and the other for the rated power region (18 m/s)—were used. Since both the conventional PI and the proposed H-infinity have the same torque schedule in the maximum power coefficient region and the transition region, the mean wind speed in the maximum power coefficient region was not used in the simulation. For the turbulence intensity, the normal turbulence model for wind turbine class IA in the IEC 61400-1 (Ed. 3) standard [23] was used. The dynamic simulation was performed for 600 s.

Figure 8 shows the time series of the two turbulent wind speeds used in the simulations. The verification of the controller was also performed with and without sensor noise signals. For the simulation in a noisy environment, random Gaussian noise was added to the signals, namely, the generator speed, the blade pitch angle, and the generator torque.

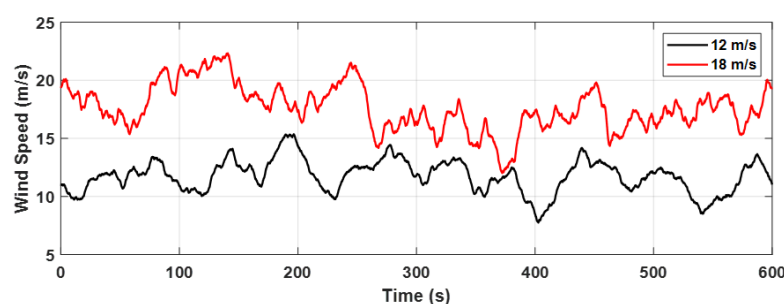


Figure 8. Time-domain diagram at 12 m/s and 18 m/s in NTM.

To verify the performance of the controller in extreme wind conditions, in addition to normal operating conditions, the extreme operating gust (EOG) wind conditions in IEC 61400-1 (Ed. 3) were used [23]. Figure 9 shows the time series of the wind speed with the two EOG wind conditions, one at 12 m/s and the other at 18 m/s, used in the simulation.

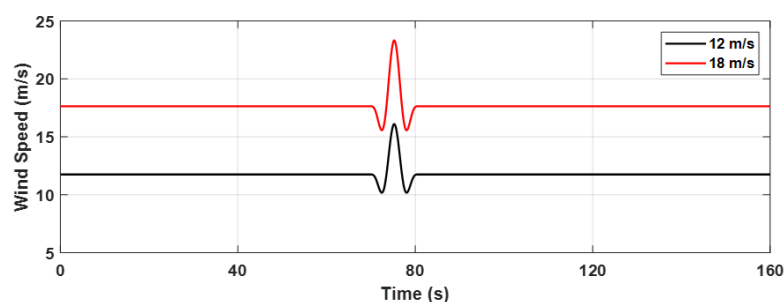


Figure 9. Time-domain diagram at 12 m/s and 18 m/s in EOG.

4.2. NTM Results in Noiseless Environments

Figure 10a,b show the simulation results of the noiseless environment in the transition region and the rated power region, respectively. The results of the two different controllers, namely, the conventional PI and the proposed pitch H-infinity, are shown in the figure. Based on the figures, the operating data of the wind turbine with two different controllers mostly appear to be similar but also show slight differences. For the transition region (12 m/s), the generator torque and the electrical power with the conventional PI algorithm include a few downward peaks, but they are slightly improved with the H-infinity control. For the rated power region, it can be found that the fluctuations in the rotor speed and the electrical power are slightly reduced with the pitch H-infinity control. Therefore, in a noiseless environment, the proposed pitch H-infinity control implemented in the

conventional control algorithms is found to work properly and to show slightly better performance in reducing fluctuations.

Tables 2 and 3 show a quantitative comparison of the performances with the conventional PI and the proposed H-infinity at the two different wind speeds considered. In evaluating the controllers' performance, the mean and standard deviation of the rotor speed and the electrical power are used as criteria because they are related to the stability of the wind turbine in operating situations.

Although they are not related to the controller performance, the mean and standard deviation of the estimated wind speed for the controllers are given in Tables 2 and 3 for comparison purposes. The wind speeds are the estimated wind speeds calculated using the wind estimator. Although the design parameters of the wind estimator are the same for the two different control algorithms under the same wind speed conditions, the wind speeds estimated are slightly different at 12 m/s and 18 m/s due to the different operating points caused by the different control algorithms.

Based on the results in Table 2, the standard deviation of the rotor speed is reduced by approximately 8% with the proposed pitch H-infinity control compared to that with the conventional PI control at an average wind speed of 12 m/s. Moreover, as shown in Table 3, the standard deviation of the generator speed is reduced by approximately 10% with the proposed H-infinity control compared with that of the PI control at an average wind speed of 18 m/s. For the mean values of the rotor speed and the electrical power, they are not significantly changed by the proposed algorithm.

As a result, Tables 2 and 3 clearly show that the rotor speed standard deviation of the pitch H-infinity controller is better than that of the conventional PI controller under the noiseless NTM conditions with average wind speeds of 12 m/s and 18 m/s.

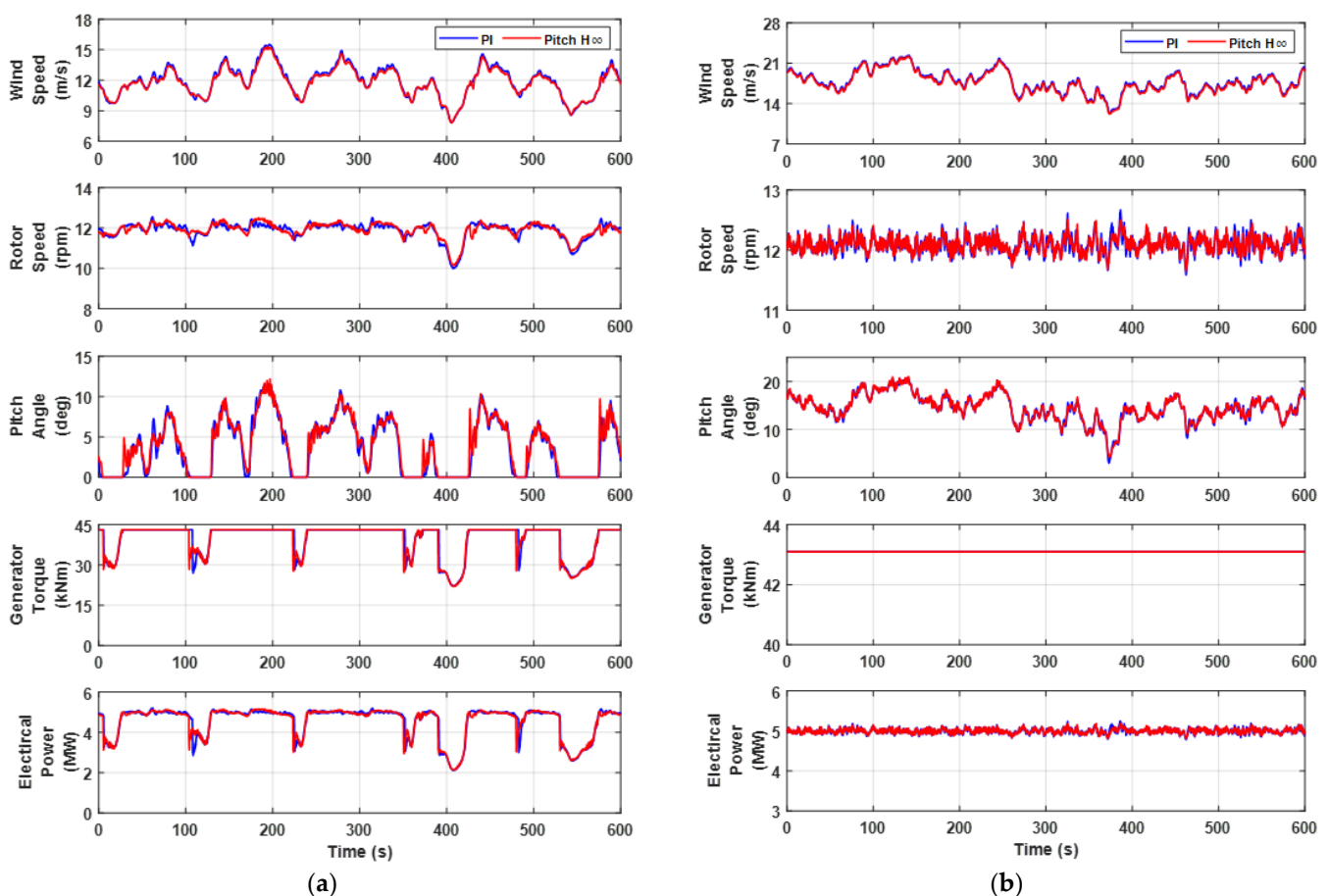


Figure 10. NTM results in noiseless environments. (a) Wind speed of 12 m/s; (b) wind speed of 18 m/s.

Table 2. Comparison of NTM results for performance data in 12 m/s noiseless environment.

Performance Data	Mean			Std. Dev.		
	PI (A)	H-Infinity (B)	(B-A)/A (%)	PI (C)	H-Infinity (D)	(D-C)/C (%)
V_{est} (m/s)	11.882	11.770	-0.94	1.527	1.417	-7.21
Ω_r (rpm)	11.891	11.907	0.13	0.412	0.379	-8.08
P (MW)	4.568	4.557	-0.24	0.778	0.767	-1.45

Table 3. Comparison of NTM results for performance data in 18 m/s noiseless environment.

Performance Data	Mean			Std. Dev.		
	PI (A)	H-Infinity (B)	(B-A)/A (%)	PI (C)	H-Infinity (D)	(D-C)/C (%)
V_{est} (m/s)	17.834	17.591	-1.36	1.935	1.952	0.90
Ω_r (rpm)	12.098	12.100	0.02	0.136	0.122	-9.98
P (MW)	4.999	5.000	0.01	0.059	0.054	-9.08

4.3. Noise Filter for NTM in Noisy Sensor Environments

In the NTM noisy environment, the conventional PI controller without a sensor noise reduction module appeared to be unable to control the wind turbine due to the sensor noise in the signal. Therefore, a filter was designed for the conventional controller and implemented. Considering that both the pitch and the torque control loops of the conventional control algorithm use the generator speed as an input signal, a finite impulse response (FIR) filter was used for the generator speed signal in the feedback loop to reduce the effect of sensor noise on the conventional PI controller.

The FIR filter used is a moving average filter that reduces the effect of sensor noise on the signal by calculating a moving average for every M step [24]. The value of M used was 30, which means that the average value was calculated for every 30 steps of the signal. The equation for the FIR filter is shown in Equation (10), where $x(n)$ and $y(n)$ are the input signal and output signal, respectively. And, m represents the feedback input signal at the m 'th instant. A block diagram of the filter is shown in Figure 11.

$$y(n) = \frac{1}{M} \sum_{m=0}^{M-1} x(n - m) \tag{10}$$

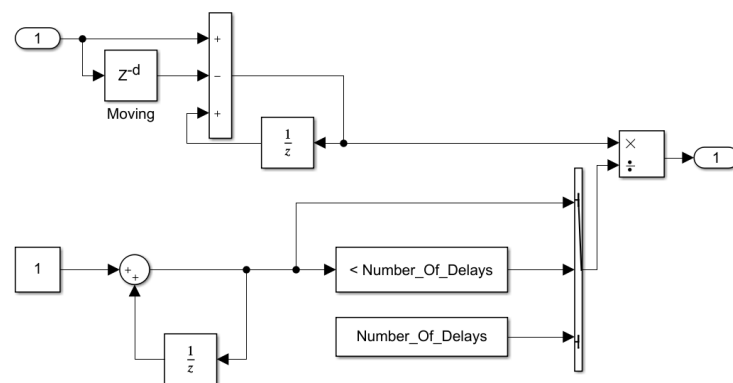


Figure 11. Block diagram of the FIR filter.

4.4. NTM Results in Noisy Environments

Figure 12a,b show the simulation results of NTM for noisy conditions in the transition regions and the rated power regions, respectively. To simulate the noisy environment, random mixing Gaussian noise was added to all feedback signals, which were the generator speed, blade pitch angle, and the generator torque. The wind speed data for the PI and the pitch H-infinity control in Figure 12 are the wind speeds estimated by the wind estimator, which contains high-frequency oscillation signals due to the white noise. The results with

the conventional control are the results with the filter described in Section 4.4, and those with the proposed H-infinity control are the results without the filter.

In Figure 12a,b, more high-frequency components are shown in the signals due to sensor noise. Downward peaks in the generator torque and the electrical power are still shown in Figure 12a, and the peaks are found to be reduced with the proposed pitch H-infinity controller. For higher wind speeds, high-frequency fluctuations in the rotor speed, blade pitch angle, and electrical power are found to be much reduced with the pitch H-infinity controller.

Tables 4 and 5 show a quantitative comparison of the performances of the conventional PI and the proposed pitch H-infinity controllers at the two different wind speeds considered. As with Tables 2 and 3, the wind speeds are the estimated values from the wind speed estimator, and they are only presented for monitoring purposes. As shown in Table 4, the mean values of the estimated wind speed, rotor speed, and electrical power were not significantly different for the simulations with the two different controllers. However, the standard deviation of the rotor speed was reduced by around 9%. This trend is similar for the rated power region; the mean values of the estimated wind speed, rotor speed, and electrical power were not significantly different for the simulations with the two different controllers, but lower standard deviations were obtained with the proposed pitch H-infinity controller. As shown in Table 5, the standard deviations of the rotor speed and the electrical power were reduced by around 30% with the pitch H-infinity controller compared to those of the PI controller.

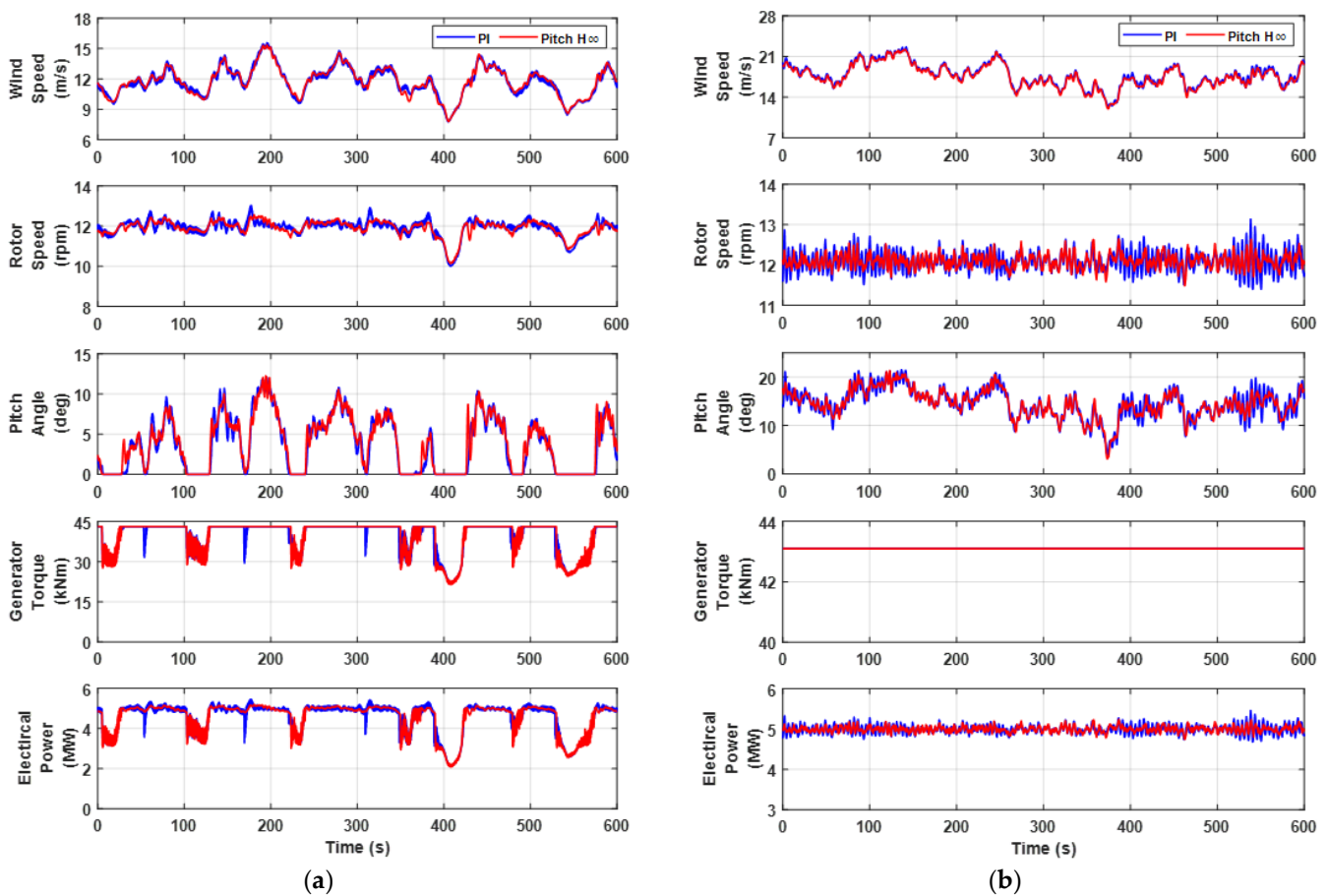


Figure 12. NTM results in noisy environments. (a) Wind speed of 12 m/s; (b) wind speed of 18 m/s.

Table 4. Comparison of NTM results for performance data in 12 m/s noisy environment.

Performance Data	Mean			Std. Dev.		
	PI (A)	H-Infinity (B)	(B-A)/A (%)	PI (C)	H-Infinity (D)	(D-C)/C (%)
V_{est} (m/s)	11.731	11.765	0.29	1.424	1.420	-0.27
Ω_r (rpm)	11.926	11.907	-0.16	0.423	0.385	-9.08
P (MW)	4.561	4.554	-0.15	0.764	0.769	0.68

Table 5. Comparison of NTM results for performance data in 18 m/s noisy environment.

Performance Data	Mean			Std. Dev.		
	PI (A)	H-Infinity (B)	(B-A)/A (%)	PI (C)	H-Infinity (D)	(D-C)/C (%)
V_{est} (m/s)	17.822	17.596	-1.27	1.952	1.963	0.57
Ω_r (rpm)	12.090	12.099	0.08	0.240	0.167	-30.62
P (MW)	4.996	5.000	0.08	0.101	0.071	-30.42

4.5. EOG Results in Noiseless Environments

Figure 13a,b show the simulation results for the transition region and the rated power region with the EOG situations, respectively. According to the wind turbine design standard of IEC 61400-1 (Ed. 3) class IA, the EOG simulations of the two controllers, i.e., the conventional PI controller and the pitch H-infinity controller, were performed with a simulation time of 160 s. As shown in the figures, the estimated wind speed, the rotor speed, and the electrical power appear to be similar in shape with the two different controllers, but the magnitude and the oscillation are found to be reduced with the pitch H-infinity controller.

Tables 6 and 7 show a quantitative comparison of the controller performance for the transition region and the rated power region with the EOG situations. As with the results with the NTM situations, the mean values of the performance data were not significantly different, but the standard deviations were reduced considerably with the pitch H-infinity controller compared with those of the conventional PI controller. For the EOG situation at 12 m/s, the standard deviations of the rotor speed and the electrical power were reduced by approximately 46%, and they were reduced by approximately 39% at 18 m/s with the pitch H-infinity controller.

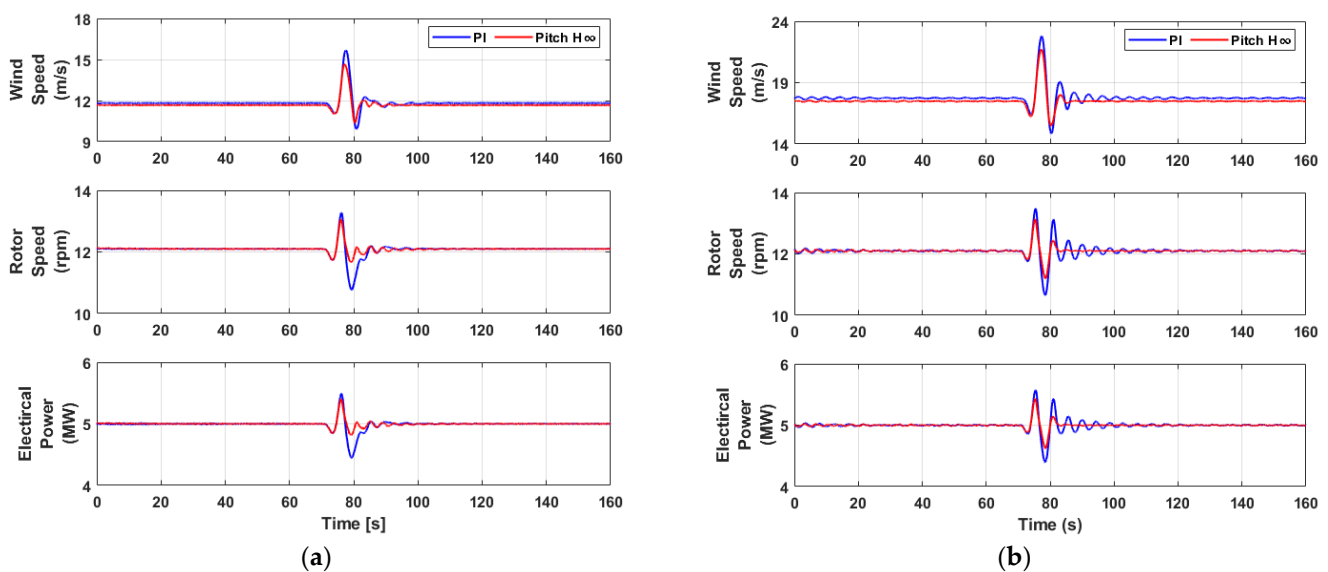
**Figure 13.** EOG results in noiseless environments. (a) Wind speed of 12 m/s; (b) wind speed of 18 m/s.

Table 6. Comparison of EOG results for performance data in 12 m/s noiseless environment.

Performance Data	Mean			Std. Dev.		
	PI (A)	H-Infinity (B)	(B-A)/A (%)	PI (C)	H-Infinity (D)	(D-C)/C (%)
V_{est} (m/s)	11.774	11.697	−0.66	0.467	0.343	−26.58
Ω_r (rpm)	12.080	12.099	0.15	0.189	0.101	−46.61
P (MW)	4.991	4.999	0.15	0.079	0.042	−46.55

Table 7. Comparison of EOG results for performance data in 18 m/s noiseless environment.

Performance Data	Mean			Std. Dev.		
	PI (A)	H-Infinity (B)	(B-A)/A (%)	PI (C)	H-Infinity (D)	(D-C)/C (%)
V_{est} (m/s)	17.658	17.514	−0.81	0.611	0.508	−16.90
Ω_r (rpm)	12.098	12.099	0.01	0.210	0.127	−39.65
P (MW)	4.999	5.000	0.01	0.088	0.053	−39.66

The simulation results clearly show that the pitch H-infinity controller performs better in the recovery time and the rotor speed standard deviation than the PI controller in the EOG situation.

5. Conclusions

In this study, a new H-infinity control algorithm for VSVP wind turbines was proposed to improve the performance of conventional PI controllers. For this, the NREL 5 MW reference wind turbine was used as a target wind turbine to verify the performance of the proposed H-infinity controller. A conventional PI controller and a moving average filter were also designed for comparison with the H-infinity control algorithm. To verify that the proposed H-infinity control can work stably with various wind conditions, an NTM model with noise, an NTM model without noise, and an EOG model without noise were simulated for the transition region of 12 m/s and the rated power region of 18 m/s.

From the NTM simulation results without considering noise, it was found that the standard deviation of the rotor speed in the transition region was reduced by 8.076% for the pitch H-infinity controller compared to the PI controller. In the rated power region, the standard deviation of the rotor speed was reduced by 9.98%. From the NTM simulation results considering noise, it was found that the conventional PI controller could not operate due to the noise, so a moving average filter for the conventional controller was designed and implemented. Compared with the conventional PI controller, the standard deviation of the rotor speed in the transition region was reduced by 9.08% with the H-infinity controller. In the rated power region, the standard deviation of the rotor speed was reduced by 30.62%.

A performance improvement by the proposed H-infinity controller was also found in the EOG simulation. The standard deviation of the rotor speed was reduced by 46.61% for the pitch H-infinity controller compared to that of the conventional PI controller in the transition region, and it was reduced by 39.65% in the rated power region.

In this study, the pitch H-infinity control algorithm was designed based on the conventional PI control algorithm, which makes the pitch H-infinity control algorithm effective in improving the rotor speed standard deviation of wind turbines in medium to high wind speed regions without affecting the power generation of wind turbines and without changing the structure of the traditional control algorithm, in both noisy and noiseless environments. Moreover, it is simpler and easier for realistic application.

Author Contributions: Conceptualization, Y.S., T.J. and B.D.; methodology, Y.S.; software, Y.S.; supervision, I.P.; validation, Y.S.; writing—original draft, Y.S.; writing—review and editing, I.P. All authors have read and agreed to the published version of the manuscript.

Funding: This work was supported by the International Energy Joint R&D Program and the Human Resources Development Program in Energy Technology and New & Renewable Energy Core Technology program of the Korea Institute of Energy Technology Evaluation and Planning (KETEP),

granted financial resource from the Ministry of Trade, Industry & Energy, Republic of Korea. (Nos. 20218530050040 and 20204030200010).

Institutional Review Board Statement: Not applicable.

Informed Consent Statement: Not applicable.

Data Availability Statement: Not applicable.

Conflicts of Interest: The authors declare no conflict of interest.

References

- IRENA. *Renewable Power Generation Costs in 2021*; International Renewable Energy Agency: Abu Dhabi, United Arab Emirates, 2022.
- Jiang, Z.; Xing, Y. Load Mitigation Method for Wind Turbines during Emergency Shutdowns. *Renew. Energy* **2022**, *185*, 978–995. [[CrossRef](#)]
- Guo, J.; Lu, S.; Zhai, C.; He, Q. Automatic Bearing Fault Diagnosis of Permanent Magnet Synchronous Generators in Wind Turbines Subjected to Noise Interference. *Meas. Sci. Technol.* **2018**, *29*, 025002. [[CrossRef](#)]
- Nam, Y. *Wind Turbine System Control*, 1st ed.; GS Interservice: Seoul, Korea, 2013.
- Bossanyi, E.A. The Design of Closed Loop Controllers for Wind Turbines. *Wind Energy* **2000**, *3*, 149–163. [[CrossRef](#)]
- Burton, T.; Jenkins, N.; Sharpe, D. *Bossanyi, Wind Energy Handbook*, 2nd ed.; John Wiley & Sons, Ltd.: Hoboken, NJ, USA, 2011; pp. 475–523. ISBN 978-1-119-99271-4.
- Engelen, T.G.V.; Hooft, E.L.V.D.; Schaak, P. *Development of Wind Turbine Control Algorithms for Industrial Use*; Netherlands Energy Research Foundation: Petten, The Netherlands, 2001.
- Engelen, T.; Markou, H.; Buhl, T.; Marrant, B. *Morphological Study of Aeroelastic Control Concepts for Wind Turbines*; EU-Contract ENK5-CT-2002-00627; ECN Report: Petten, The Netherlands, 2006.
- Lio, W.H.A. *Blade-Pitch Control for Wind Turbine Load Reductions*; Springer: Berlin/Heidelberg, Germany, 2018; ISBN 978-3-319-75532-8.
- Kim, C.; Kim, K.; Song, Y.; Paek, I. Tower load reduction control by pitch loop individual gain scheduling. *J. Wind Energy* **2018**, *9*, 25–32.
- Oh, Y.; Kim, K.; Kim, H.; Paek, I. Control Algorithm of a Floating Wind Turbine for Reduction of Tower Loads and Power Fluctuation. *Int. J. Precis. Eng. Manuf.* **2015**, *16*, 2041–2048. [[CrossRef](#)]
- Kim, K.; Paek, I.; Kim, C.; Kim, H.; Kim, H. Design of Power and Load Reduction Controller for a Medium-Capacity Wind Turbine. *J. Korean Sol. Energy Soc.* **2016**, *36*, 1–12. [[CrossRef](#)]
- Kim, C.; Kim, K.; Paek, I. Design of tower damper gain scheduling algorithm for wind turbine tower load reduction. *J. Korean Sol. Energy Soc.* **2018**, *38*, 1–13. [[CrossRef](#)]
- Moradi, H.; Vossoughi, G. Robust Control of the Variable Speed Wind Turbines in the Presence of Uncertainties: A Comparison between H-infinity and PID Controllers. *Energy* **2015**, *90*, 1508–1521. [[CrossRef](#)]
- Pourseif, T.; Atuwwo, T.; Doniqi, S.A.; Andani, M.T.; Yousefpour, K.; Pourgharibshahi, H.; Ramezani, Z. Design of H-Infinity Controller for Wind Turbine in the Cold Weather Conditions. In Proceedings of the 2018 Clemson University Power Systems Conference (PSC), Charleston, SC, USA, 4–7 September 2018; pp. 1–6.
- De Corcuera, A.D.; Pujana-Arrese, A.; Ezquerro, J.M.; Seguro, E.; Landaluze, J. H-infinity Based Control for Load Mitigation in Wind Turbines. *Energies* **2012**, *5*, 938–967. [[CrossRef](#)]
- Surinkaew, T.; Ngamroo, I. Robust Power Oscillation Damper Design for DFIG-Based Wind Turbine Based on Specified Structure Mixed H2/H-infinity Control. *Renew. Energy* **2014**, *66*, 15–24. [[CrossRef](#)]
- Yao, X.; Guo, C.; Li, Y. LPV H-Infinity Controller Design for Variable-Pitch Variable-Speed Wind Turbine. In Proceedings of the 2009 IEEE 6th International Power Electronics and Motion Control Conference, Wuhan, China, 17–20 May 2009; pp. 2222–2227.
- Jonkman, J.; Butterfield, S.; Musial, W.; Scott, G. *Definition of a 5-MW Reference Wind Turbine for Offshore System Development*; National Renewable Energy Lab. (NREL): Golden, CO, USA, 2009.
- Kim, K.; Kim, H.-G.; Paek, I. Application and Validation of Peak Shaving to Improve Performance of a 100 KW Wind Turbine. *Int. J. Precis. Eng. Manuf.—Green Technol.* **2020**, *7*, 411–421. [[CrossRef](#)]
- Zhou, K.; Doyle, J.C.; Glover, K. *Robust and Optimal Control*, 1st ed.; Pearson: Upper Saddle River, NJ, USA, 1995; ISBN 978-0-13-456567-5.
- Kim, K.; Kim, H.-G.; Song, Y.; Paek, I. Design and Simulation of an LQR-PI Control Algorithm for Medium Wind Turbine. *Energies* **2019**, *12*, 2248. [[CrossRef](#)]
- IEC (International Electrotechnical Commission). *Wind Turbines—Part 1: Design Requirements*, 3rd ed.; IEC 61400-1; International Electrotechnical Commission: Geneva, Switzerland, 2019.
- Oshana, R. Overview of DSP Algorithms. In *DSP for Embedded and Real-Time Systems*; Oshana, R., Ed.; Newnes: Oxford, UK, 2012; pp. 113–131. ISBN 978-0-12-386535-9.